



MOX-Report No. 53/2021

**On the effect of boundary conditions on the scalability
of Schwarz methods**

Ciaramella, G.; Mechelli, L.

MOX, Dipartimento di Matematica
Politecnico di Milano, Via Bonardi 9 - 20133 Milano (Italy)

mox-dmat@polimi.it

<http://mox.polimi.it>

On the effect of boundary conditions on the scalability of Schwarz methods

Gabriele Ciaramella and Luca Mechelli

1 Introduction

This work is concerned with convergence and weak scalability¹ analysis of one-level parallel Schwarz method (PSM) and optimized Schwarz method (OSM) for the solution of the problem

$$\begin{aligned} -\Delta u &= f \text{ in } \Omega, & u(a_1, y) &= u(b_N, y) = 0 \quad y \in (0, 1), \\ \mathcal{B}_b(u)(x) &= \mathcal{B}_t(u)(x) = 0 & x &\in (a_1, b_N), \end{aligned} \quad (1)$$

where Ω is the domain depicted in Fig. 1, and \mathcal{B}_b and \mathcal{B}_t are either Dirichlet, or Neumann or Robin operators:

$$\begin{aligned} \text{Dirichlet: } \mathcal{B}_b(u)(x) &= u(0, x), & \mathcal{B}_t(u)(x) &= u(1, x), \\ \text{Neumann: } \mathcal{B}_b(u)(x) &= \partial_y u(0, x), & \mathcal{B}_t(u)(x) &= \partial_y u(1, x), \\ \text{Robin: } \mathcal{B}_b(u)(x) &= qu(0, x) - \partial_y u(0, x), & \mathcal{B}_t(u)(x) &= qu(1, x) + \partial_y u(1, x). \end{aligned}$$

Here, $q > 0$ and the subscripts ‘ b ’ and ‘ t ’ stand for ‘bottom’ and ‘top’. As shown in Fig. 1, the domain Ω is the union of subdomains Ω_j , $j = 1, \dots, N$, defined as $\Omega_j := (a_j, b_j) \times (0, 1)$, where $a_1 = 0$, $a_j = L + a_{j-1}$ for $j = 2, \dots, N + 1$ and $b_j = a_{j+1} + 2\delta$ for $j = 0, \dots, N$. Hence, the length of each subdomain is $L + 2\delta$ and the length of the overlap is 2δ with $\delta \in (0, L/2)$.

It is well known that one-level Schwarz methods are not weakly scalable, if the number of subdomains increases and the whole domain Ω is fixed. How-

Gabriele Ciaramella
Politecnico di Milano e-mail: gabriele.ciaramella@polimi.it

Luca Mechelli
Universität Konstanz e-mail: luca.mechelli@uni-konstanz.de

¹ Here, weak scalability is understood in the sense that the contraction factor does not deteriorate as the number N of subdomains increases and, hence, the number of iterations, needed to reach a given tolerance, is uniformly bounded in N ; see, e.g., [3].

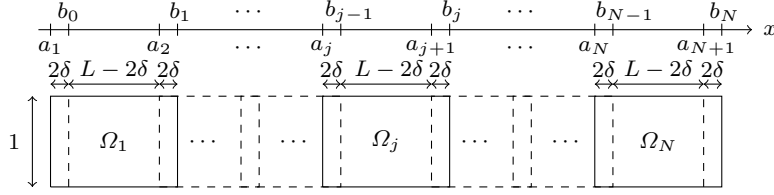


Fig. 1 Two-dimensional chain of N rectangular fixed-sized subdomains.

ever, the recent work [2], published in the field of implicit solvation models used in computational chemistry, has drawn attention to the opposite case in which the number of subdomains increases, but their size remains unchanged, and, as a result, the size of the whole domain Ω increases. In this setting, weak scalability of PSM and OSM for (1) with Dirichlet boundary conditions is studied in [4, 3]. Scalability results for the PSM in case of more general geometries of the (sub)domains are presented in [5, 6, 7]. In these works, only external Dirichlet conditions are discussed and, in such a case, weak scalability is shown; see also [11] for a scalability analysis of the classical (alternating) Schwarz method. A short remark about the non-scalability in case of external Neumann conditions is given in [3]. Similar results have been recently presented in [1] for time-harmonic problems. Moreover, very similar results to the ones of [3] are obtained a few years later in [9]. The goal of this work is to study the effect of different (possibly mixed) external boundary conditions on convergence and scalability of PSM and OSM. In particular, we will show that only in the case of (both) external Neumann conditions at the top and the bottom of Ω , PSM and OSM are not scalable. External Dirichlet conditions lead to the fastest convergence, while external Robin conditions lead to a convergence that depends heavily on the parameter q .

One-level PSM and OSM for the solution of (1) are

$$\begin{aligned}
 -\Delta u_j^n &= f_j \text{ in } \Omega_j, \\
 \mathcal{B}_b(u_j^n)(x) &= \mathcal{B}_t(u_j^n)(x) = 0 \quad x \in (a_1, b_N), \\
 \mathcal{T}_\ell(u_j^n)(a_j) &= \mathcal{T}_\ell(u_{j-1}^{n-1})(a_j), \quad \mathcal{T}_r(u_j^n)(b_j) = \mathcal{T}_r(u_{j+1}^{n-1})(b_j),
 \end{aligned} \tag{2}$$

for $j = 1, \dots, N$, where \mathcal{T}_ℓ and \mathcal{T}_r are Dirichlet trace operators,

$$\mathcal{T}_\ell(u_j^n)(a_j) = u_j^n(a_j, y) \text{ and } \mathcal{T}_r(u_j^n)(b_j) = u_j^n(b_j, y), \tag{3}$$

for the PSM, and Robin trace operators,

$$\mathcal{T}_\ell(u_j^n)(a_j) = pu_j^n(a_j, y) - \partial_x u_j^n(a_j, y) \text{ and } \mathcal{T}_r(u_j^n)(b_j) = pu_j^n(b_j, y) + \partial_x u_j^n(b_j, y), \tag{4}$$

with $p > 0$ for the OSM. The subscript ‘ ℓ ’ and ‘ r ’ stand for ‘left’ and ‘right’. For $j = 1$ the condition at a_1 must be replaced by $u_1^n(a_1, y) = 0$ and for $j = N$ the condition at b_N must be replaced by $u_N^n(b_N, y) = 0$. In this

paper, ‘external conditions’ and ‘transmission conditions’ will always refer to the conditions obtained by the pairs $(\mathcal{B}_b, \mathcal{B}_u)$ and $(\mathcal{T}_\ell, \mathcal{T}_r)$, respectively. Note that the Robin parameter p of the OSM can be chosen independently of the Robin parameter q used for the operators \mathcal{B}_b and \mathcal{B}_t . We analyze convergence of PSM and OSM by a Fourier analysis in Section 3. For this purpose, we use the solutions of eigenproblems of the 1D Laplace operators with mixed boundary conditions. These are studied in Section 2. Finally, results of numerical experiments are presented in Section 4.

2 Laplace eigenpairs for mixed external conditions

Consider the 1D eigenvalue problem

$$\varphi''(y) = -\lambda\varphi(y), \text{ for } y \in (0, 1), \quad \mathcal{B}_b(\varphi)(0) = \mathcal{B}_t(\varphi)(1) = 0, \quad (5)$$

and six pairs of boundary operators $(\mathcal{B}_b, \mathcal{B}_t)$:

$$\begin{aligned} \text{(DD)} \quad & \mathcal{B}_b(\varphi)(0) = \varphi(0), & \mathcal{B}_t(\varphi)(1) &= \varphi(1), \\ \text{(DR)} \quad & \mathcal{B}_b(\varphi)(0) = \varphi(0), & \mathcal{B}_t(\varphi)(1) &= q\varphi(1) + \varphi'(1), \\ \text{(DN)} \quad & \mathcal{B}_b(\varphi)(0) = \varphi(0), & \mathcal{B}_t(\varphi)(1) &= \varphi'(1), \\ \text{(RR)} \quad & \mathcal{B}_b(\varphi)(0) = q\varphi(0) - \varphi'(0), & \mathcal{B}_t(\varphi)(1) &= q\varphi(1) + \varphi'(1), \\ \text{(NR)} \quad & \mathcal{B}_b(\varphi)(0) = \varphi'(0), & \mathcal{B}_t(\varphi)(1) &= q\varphi(1) + \varphi'(1), \\ \text{(NN)} \quad & \mathcal{B}_b(\varphi)(0) = \varphi'(0), & \mathcal{B}_t(\varphi)(1) &= \varphi'(1), \end{aligned}$$

where $q > 0$ and ‘D’, ‘R’ and ‘N’ stand for ‘Dirichlet’, ‘Robin’ and ‘Neumann’. For all these six cases the eigenvalue problem (5) is solved by orthonormal (in $L^2(0, 1)$) Fourier basis functions.

Theorem 1 (Eigenpairs of the Laplace operator)

Let $q > 0$. The eigenproblems (5) with the above external conditions are solved by the non-trivial eigenpairs (φ_k, λ_k) given by

$$\begin{aligned} \text{(DD)} \quad & \varphi_k(y) = \sqrt{2} \sin(\pi k y), \quad \lambda_k = \pi^2 k^2, \quad k = 1, 2, \dots \\ \text{(DR)} \quad & \varphi_k(y) = \sqrt{\frac{4\mu_k}{2\mu_k - \sin(2\mu_k)}} \sin(\mu_k y), \quad \lambda_k = \mu_k^2, \quad k = 1, 2, \dots, \text{ where} \\ & \mu_k \in (k\pi - \pi/2, k\pi), \quad k = 1, 2, \dots, \text{ are roots of } \widehat{d}(x) := q \sin(x) + x \cos(x). \text{ Moreover, } \lim_{q \rightarrow 0} \mu_1(q) = \pi/2 \text{ and } \lim_{q \rightarrow \infty} \mu_1(q) = \pi. \\ \text{(DN)} \quad & \varphi_k(y) = \sqrt{2} \sin\left(\frac{2k+1}{2} \pi y\right), \quad \lambda_k = \frac{(2k+1)^2}{4} \pi^2, \quad k = 0, 1, 2, \dots \\ \text{(RR)} \quad & \varphi_k(y) = \sqrt{\frac{4\tau_k}{(\tau_k^2 - q^2) \sin(2\tau_k) + 4q\tau_k \sin(\tau_k)^2 + 2\tau_k^3 + 2q^2\tau_k}} (q \sin(\tau_k y) + \tau_k \cos(\tau_k y)), \\ & \lambda_k = \tau_k^2, \quad k = 1, 2, \dots, \text{ where } \tau_k \in (0, \pi), \quad k = 1, 2, \dots, \text{ are roots of} \\ & \widetilde{d}(x) := 2qx \cos(x) + (q^2 - x^2) \sin(x). \text{ Moreover, } \lim_{q \rightarrow 0} \tau_1(q) = 0 \text{ and} \\ & \lim_{q \rightarrow \infty} \tau_1(q) = \pi. \\ \text{(NR)} \quad & \varphi_k(y) = \sqrt{\frac{4\nu_k}{2\nu_k + \sin(2\nu_k)}} \cos(\nu_k y), \quad \lambda_k = \nu_k^2, \quad k = 1, 2, \dots, \text{ where} \\ & \nu_k \in ((k-1)\pi, (k-\frac{1}{2})\pi), \quad k = 1, 2, \dots, \text{ are roots of } d(x) := x \sin(x) - q \cos(x). \text{ Moreover, } \lim_{q \rightarrow 0} \nu_1(q) = 0 \text{ and } \lim_{q \rightarrow \infty} \nu_1(q) = \pi/2. \end{aligned}$$

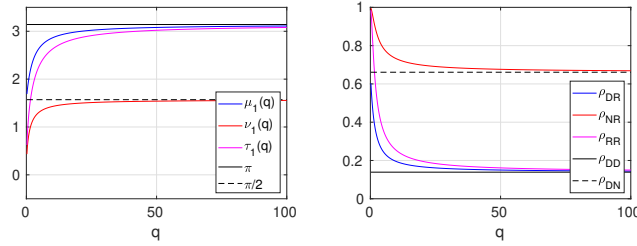


Fig. 2 Left: Maps $q \mapsto \mu_1(q)$, $q \mapsto \nu_1(q)$ and $q \mapsto \tau_1(q)$. Right: ρ_{DR} , ρ_{NR} , ρ_{DD} and ρ_{DN} as functions of q and for $\delta = 0.1$ and $L = 1.0$.

$$(NN) \quad \varphi_k(y) = \sqrt{2} \cos(\pi k y), \quad \lambda_k = \pi^2 k^2, \quad k = 0, 1, 2, \dots$$

Proof If we multiply (5) with φ , integrate over $[0, 1]$, and integrate by parts, we get $\lambda \int_0^1 |\varphi(y)|^2 dy = \int_0^1 |\varphi'(y)|^2 dy - \varphi'(1)\varphi(1) + \varphi'(0)\varphi(0)$. Using any of the above external conditions (and that $q > 0$, for the Robin ones) one gets $\lambda \geq 0$. We refer to, e.g., [10, Section 4.1] for similar discussions. Now, all the cases can be proved by using the ansatz $\varphi(y) = A \cos(\sqrt{\lambda}y) + B \sin(\sqrt{\lambda}y)$, which clearly satisfies (5), and computing, e.g., A and λ in such a way that $\varphi(y)$ satisfies the two external conditions and B as a normalization factor. \square

The coefficients ν_1 , μ_1 and τ_1 as functions of q are shown in Fig. 2 (left), where we can observe that $\nu_1(q) < \frac{\pi}{2} < \mu_1(q) < \pi$ and $0 < \tau_1(q) < \pi$, and that the maps $q \mapsto \nu_1(q)$, $q \mapsto \mu_1(q)$ and $q \mapsto \tau_1(q)$ increase monotonically and approach, respectively, $\frac{\pi}{2}$ and π as $q \rightarrow \infty$. Hence, by taking the limit $q \rightarrow 0$, one can pass from the conditions (DR), (RR) and (NR) to (DN), (NN) and (NN), respectively. Similarly, by taking the limit $q \rightarrow \infty$, the conditions (DR), (RR) and (NR) become (DD), (DD) and (DN), respectively.

3 Convergence and scalability

Consider the Schwarz method (2) and any pair $(\mathcal{B}_b, \mathcal{B}_t)$ of operators as in Section 2. The Fourier expansions of $u_j^n(x, y)$, $j = 1, \dots, N$, are

$$u_j^n(x, y) = \sum_k \hat{u}_j^n(x, \lambda_k) \varphi_k(y), \quad (6)$$

where the sum is over $k = 1, 2, \dots$ for (DD), (DR), (RR) and (NR), and over $k = 0, 1, 2, \dots$ for (DN) and (NN). The functions φ_k depend on the external boundary conditions and are the ones obtained in Theorem 1. The Fourier coefficients $\hat{u}_j^n(x, \lambda_k)$ satisfy²

² Notice that the procedure to obtain (7) is standard. We refer to, e.g., [10] for more details and examples.

$$\begin{aligned}
 -\partial_{xx}\widehat{u}_j^n(x, \lambda_k) + \lambda_k\widehat{u}_j^n(x, \lambda_k) &= \widehat{f}_j(x, \lambda_k) \text{ in } (a_j, b_j), \\
 \mathcal{T}_\ell(\widehat{u}_j^n(\cdot, \lambda_k))(a_j) &= \mathcal{T}_\ell(\widehat{u}_{j-1}^{n-1}(\cdot, \lambda_k))(a_j), \\
 \mathcal{T}_r(\widehat{u}_j^n(\cdot, \lambda_k))(b_j) &= \mathcal{T}_r(\widehat{u}_{j+1}^{n-1}(\cdot, \lambda_k))(b_j),
 \end{aligned} \tag{7}$$

for $j = 1, \dots, N$. For $j = 1$, the condition at a_1 must be replaced by $u_1^n(a_1) = 0$ and for $j = N$ the condition at b_N must be replaced by $u_N^n(b_N) = 0$. If the operators \mathcal{T}_ℓ and \mathcal{T}_r correspond to Dirichlet conditions (see (3)), then (7) is a PSM. If they correspond to Robin conditions (see (4)), then (7) is an OSM. The convergence of the iteration (7) is analyzed in Theorem 2.

Theorem 2 (Convergence of Schwarz methods in Fourier space)

The contraction factors of the Schwarz methods³ (7) are bounded by

$$\rho(\lambda_k, \delta) = \frac{e^{2\lambda_k\delta} + e^{\lambda_k L}}{e^{2\lambda_k\delta + \lambda_k L} + 1}. \tag{8}$$

Moreover, it holds that $\rho(\lambda_k, \delta) \in [0, 1]$ with $\rho(0, \delta) = 1$ (independently of N), and that $\lambda \mapsto \rho(\lambda, \delta)$ is strictly monotonically decreasing.

Proof The Dirichlet case follows from [4, Lemma 2 and Theorem 3]. See also [3, Lemma 2 and Theorem 1]. We focus here on the Robin case. From Theorem 3 in [3] and the corresponding proof we have that the contraction factor of the OSM is bounded by $\max\{\varphi(\lambda, \delta, p), |\zeta(\lambda, \delta, p)|\}$ where

$$\begin{aligned}
 \varphi(\lambda, \delta, p) &:= \frac{(\lambda + p)^2 e^{2\delta\lambda} - (\lambda - p)^2 e^{-2\delta\lambda} + (\lambda + p)|\lambda - p|(e^{\lambda L} - e^{-\lambda L})}{(\lambda + p)^2 e^{\lambda L + 2\lambda\delta} - (\lambda - p)^2 e^{-\lambda L - 2\lambda\delta}} \geq 0, \\
 \zeta(\lambda, \delta, p) &:= \frac{(\lambda + p)e^{-\lambda L} + (\lambda - p)e^{\lambda L}}{(\lambda + p)e^{\lambda(L+2\delta)} + (\lambda - p)e^{-\lambda(L+2\delta)}},
 \end{aligned}$$

with $\varphi(\lambda, \delta, p) \leq \varphi(\lambda, \delta, 0) = \lim_{\tilde{p} \rightarrow \infty} \varphi(\lambda, \delta, \tilde{p}) = \frac{e^{2\delta\lambda} - e^{-2\delta\lambda} + e^{\lambda L} - e^{-\lambda L}}{e^{\lambda L + 2\delta\lambda} - e^{-\lambda L - 2\delta\lambda}}$ for all $\lambda \geq 0$ and $\delta > 0$. If we compute the derivative of $\lambda \mapsto \varphi(\lambda, \delta, 0)$ we get

$$\partial_\lambda \varphi(\lambda, \delta, 0) = -\frac{L(e^{4\delta\lambda + L\lambda} - e^{L\lambda}) + 2\delta(e^{2\delta\lambda + 2L\lambda} - e^{2\delta\lambda})}{(e^{2\delta\lambda + L\lambda} + 1)^2},$$

which is negative for any $\lambda \geq 0$ and $\delta > 0$. Thus, $\lambda \mapsto \varphi(\lambda, \delta, 0)$ is strictly monotonically decreasing. Let us now study the function $\zeta(\lambda, \delta, p)$. Direct calculations reveal that $\partial_p \zeta(\lambda, \delta, p) = -\frac{2\lambda e^{2\delta\lambda}(e^{4\lambda(\delta+L)} - 1)}{((\lambda+p)e^{4\delta\lambda+2L\lambda+\lambda-p})^2}$, which is negative for any $\lambda \geq 0$ and $\delta > 0$, and $\zeta(\lambda, \delta, 0) = \frac{(e^{2L\lambda} + 1)e^{2\delta\lambda}}{e^{4\delta\lambda+2L\lambda} + 1} > 0$ and $\lim_{p \rightarrow \infty} \zeta(\lambda, \delta, p) = -\frac{(e^{2L\lambda} - 1)e^{2\delta\lambda}}{e^{4\delta\lambda+2L\lambda} - 1} < 0$ for any $\lambda \geq 0$ and $\delta > 0$. These observations imply that $p \mapsto \zeta(\lambda, \delta, p)$ is strictly monotonically decreasing and attains its maximum at $p = 0$. Finally, a direct comparison shows that

³ The contraction factor for (7) (corresponding to the k -th Fourier component) is the spectral radius of the Schwarz iteration matrix; see [4, 3].

$\varphi(\lambda, \delta, 0) \geq \zeta(\lambda, \delta, 0) \geq \lim_{p \rightarrow \infty} |\zeta(\lambda, \delta, p)|$ and the result follows, because $\varphi(\lambda, \delta, 0) = \frac{e^{2\delta\lambda} - e^{-2\delta\lambda} + e^{\lambda L} - e^{-\lambda L}}{e^{\lambda L + 2\delta\lambda} - e^{-\lambda L - 2\delta\lambda}} = \frac{e^{2\lambda\delta} + e^{\lambda L}}{e^{2\lambda\delta + \lambda L} + 1}$. \square

Theorem 2 gives the same bound (8) for the convergence factors of PSM and OSM. This fact is not surprising. First, it is well known that OSM converges faster than PSM for $\delta > 0$. Hence, a convergence bound for the PSM is a valid bound also for the OSM. Second, in the above proof the convergence bound for the OSM is obtained for $p \rightarrow \infty$, which corresponds to passing from Robin transmission conditions to Dirichlet transmission conditions. The bound (8) is based on the ones obtained in [4, 3]. These are quite sharp for large values of N ; see, e.g., [3, Fig. 4 and Fig. 5].

We can now prove our main convergence result, which allows us to study convergence and scalability of PSM and OSM for all the external conditions considered in Section 2.

Theorem 3 (Convergence of PSM and OSM)

The contraction factors (in the L^2 norm) of PSM and OSM for the solution to (1) are bounded by

$$\begin{aligned} \text{(DD)} \quad \rho_{\text{DD}}(\delta) &:= \rho(\pi^2, \delta), & \text{(DR)} \quad \rho_{\text{DR}}(\delta, q) &:= \rho(\mu_1(q)^2, \delta), \\ \text{(DN)} \quad \rho_{\text{DN}}(\delta) &:= \rho(\pi^2/4, \delta), & \text{(RR)} \quad \rho_{\text{RR}}(\delta, q) &:= \rho(\tau_1(q)^2, \delta), \\ \text{(NR)} \quad \rho_{\text{NR}}(\delta, q) &:= \rho(\nu_1(q)^2, \delta), & \text{(NN)} \quad \rho_{\text{NN}}(\delta) &:= \rho(0, \delta) = 1, \end{aligned}$$

where $q \in (0, \infty)$ and $\rho(\lambda, \delta)$ is defined in Theorem 2. Moreover, for any $\delta > 0$ we have that

$$\rho_{\text{DD}}(\delta) < \rho_{\text{DR}}(\delta, q) < \rho_{\text{DN}}(\delta) < \rho_{\text{NR}}(\delta, q) < \rho_{\text{NN}}(\delta) = 1, \quad (9)$$

$$\rho_{\text{DD}}(\delta) < \rho_{\text{RR}}(\delta, q) < \rho_{\text{NN}}(\delta) = 1. \quad (10)$$

Proof According to Theorem 2, the bounds of the Fourier contraction factor $\rho(\lambda, \delta)$ is monotonically decreasing in λ . Therefore, an upper bound for the convergence factor of PSM and OSM (in the L^2 norm) can be obtained by taking the maximum over the admissible Fourier frequencies λ_k and invoking Parseval's identity (see, e.g., [4]). Recalling Theorem 1, these maxima are attained at $\lambda_1 = \pi^2$ for (DD), $\lambda_1 = \mu_1^2$ for (DR), $\lambda_0 = \pi^2/4$ for (DN), $\lambda_1 = \tau_1^2$ for (RR), $\lambda_1 = \nu_1^2$ for (NR), and $\lambda_0 = 0$ for (NN). The inequalities (9) and (10) follow from the monotonicity $\lambda \mapsto \rho(\lambda, \delta)$ and the fact that $\nu_1(q) < \frac{\pi}{2} < \mu_1(q) < \pi$ and $\tau_1(q) \in (0, \pi)$. \square

The inequalities (9) and (10) imply that the contraction factor is bounded, independently of N , by a constant strictly smaller than 1 for all the cases except (NN). In the case (NN), the first Fourier frequency is $\lambda_0 = 0$. Hence, the coefficients $\widehat{u}_j^n(x, \lambda_0)$ are generated by the 1D Schwarz method

$$\begin{aligned} -\partial_{xx}\widehat{u}_j^n(x, \lambda_0) &= \widehat{f}_j(x, \lambda_0) \quad \text{in } (a_j, b_j), \\ \mathcal{T}_\ell(\widehat{u}_j^n(\cdot, \lambda_0))(a_j) &= \mathcal{T}_\ell(\widehat{u}_{j-1}^{n-1}(\cdot, \lambda_0))(a_j), \\ \mathcal{T}_r(\widehat{u}_j^n(\cdot, \lambda_0))(b_j) &= \mathcal{T}_r(\widehat{u}_{j+1}^{n-1}(\cdot, \lambda_0))(b_j), \end{aligned} \quad (11)$$

$\begin{array}{c} \text{top} \\ \text{bottom} \end{array}$	Dirichlet	Robin	Neumann	$\begin{array}{c} \text{top} \\ \text{bottom} \end{array}$	Dirichlet	Robin	Neumann
Dirichlet	yes	yes	yes	Dirichlet	-	yes	-
Robin	yes	yes	yes	Robin	yes	no	no
Neumann	yes	yes	no	Neumann	-	no	-

Table 1 Left: Scalability of PSM and OSM for different external conditions (for a fixed and finite $q > 0$) applied at the top and at the bottom of the domain. Right: Robustness of PSM and OSM with respect to $q \in [0, \infty]$.

which is known to be not scalable; see, e.g., [3, 8]. The scalability of PSM and OSM for different external conditions applied at the top and at the bottom of the domain is summarized in Table 1. Inequalities (9) and (10) lead to another interesting observation. The contraction factors are clearly influenced by the external boundary conditions. Dirichlet conditions lead to faster convergence than Robin conditions, which in turn lead to faster convergence than Neumann conditions. For example, if one external condition is of the Dirichlet type, then PSM and OSM converge faster if the other condition is of the Dirichlet type and slower if this is of Robin and even slower for the Neumann type. The case (RR) is slightly different, because the corresponding convergence of PSM and OSM depends heavily on the Robin parameter q . The behavior of the bounds $\rho_{RR}(\delta, q)$, $\rho_{DR}(\delta, q)$ and $\rho_{NR}(\delta, q)$ with respect to q is depicted in Fig. 2 (right), which shows the bounds discussed in Theorem 3 as functions of q (recall that $\rho_{NN} = 1$). Here, we can observe that the inequalities (9) and (10) are satisfied and that

- As q increases the Dirichlet part of the Robin external condition dominates. In addition, the bounds ρ_{RR} and ρ_{DR} decrease and approach ρ_{DD} as $q \rightarrow \infty$. Similarly, ρ_{NR} decreases and approaches ρ_{DN} .
- As q decreases the Neumann part of the Robin external condition dominates. In addition, the bounds ρ_{NR} and ρ_{RR} decrease and approach $\rho_{NN} = 1$ as $q \rightarrow 0$. Similarly, ρ_{DR} increases and approaches ρ_{DN} .

These observations lead to Tab. 1 (right), where we summarize the robustness of PSM and OSM with respect to the parameter q . The methods are robust with respect to q only if one of the two external boundary conditions is of Dirichlet type. This is due to the fact that Robin conditions become Neumann conditions for $q \rightarrow 0$.

4 Numerical experiments

In this section, we test the scalability of PSM and OSM by numerical simulations. For this purpose, we run PSM and OSM for all the external boundary conditions discussed in this paper and measure the number of iterations required to reach a tolerance on the error of 10^{-6} . To guarantee that the initial errors contain all frequencies, the methods are initialized with random initial guesses. In all cases, each subdomain is discretized with a uniform grid of

N	DD	DR(10)	DN	RR(10)	NR(10)	NN	RR(0.1)
3	12 - 9	13 - 10	27 - 19	14 - 10	26 - 19	77 - 54	65 - 45
4	13 - 9	14 - 10	29 - 21	15 - 11	29 - 21	130 - 90	95 - 66
5	13 - 9	14 - 10	31 - 22	15 - 11	31 - 22	194 - 134	124 - 86
10	13 - 10	14 - 10	33 - 24	15 - 11	34 - 24	>401 - >401	227 - 155
30	13 - 10	14 - 10	34 - 24	15 - 11	35 - 24	>401 - >401	311 - 210
50	13 - 10	14 - 10	34 - 24	15 - 11	35 - 24	>401 - >401	319 - 216

Table 2 Number of iterations of PSM (left) and OSM (right) needed to reduce the norm of the error below a tolerance of 10^{-6} for increasing number N of fixed-sized subdomains. The maximum number of allowed iterations is 401. This limit is only reached in the (NN) case, for which PSM and OSM are not scalable.

size 90 interior points in direction x and 50 interior points in direction y . The mesh size is $h = \frac{L}{51}$, with $L = 1$, and the overlap parameter is $\delta = 10h$. For the OSM the robin parameter is $p = 10$. The Robin parameter q of the external Robin conditions is $q = 10$, and the (RR) case is also tested with $q = 0.1$. The results of our experiments are shown in Tab. 2 and confirm the theoretical results discussed in the previous sections.

References

1. N. Bootland, V. Dolean, A. Kyriakis, and J. Pestana. Analysis of parallel Schwarz algorithms for time-harmonic problems using block Toeplitz matrices. *arXiv.2006.08801*, 2020.
2. E. Cancès, Y. Maday, and B. Stamm. Domain decomposition for implicit solvation models. *J. Chem. Phys.*, 139:054111, 2013.
3. F. Chaouqui, G. Ciaramella, M. J. Gander, and T. Vanzan. On the scalability of classical one-level domain-decomposition methods. *Vietnam J. Math.*, 46(4):1053–1088, 2018.
4. G. Ciaramella and M. J. Gander. Analysis of the parallel Schwarz method for growing chains of fixed-sized subdomains: Part I. *SIAM J. Numer. Anal.*, 55(3):1330–1356, 2017.
5. G. Ciaramella and M. J. Gander. Analysis of the parallel Schwarz method for growing chains of fixed-sized subdomains: Part II. *SIAM J. Numer. Anal.*, 56(3):1498–1524, 2018.
6. G. Ciaramella and M. J. Gander. Analysis of the parallel Schwarz method for growing chains of fixed-sized subdomains: Part III. *Electron. Trans. Numer. Anal.*, 49:210–243, 2018.
7. G. Ciaramella, M. Hassan, and B. Stamm. On the scalability of the parallel Schwarz method in one-dimension. In *Domain Decomposition Methods in Science and Engineering XXV*, pages 151–158. Springer International Publishing, 2020.
8. G. Ciaramella, M. Hassan, and B. Stamm. On the scalability of the Schwarz method. *SMAI-JCM*, 6:33–68, 2020.
9. M. El Haddad, J. C. Garay, F. Magoulès, and D. B. Szyld. Synchronous and asynchronous optimized schwarz methods for one-way subdivision of bounded domains. *Numer. Linear Algebra Appl.*, 27(2), 2020.
10. P. J. Olver. *Introduction to Partial Differential Equations*. Undergraduate Texts in Mathematics. Springer International Publishing, 2013.
11. A.d Reusken and B. Stamm. Analysis of the schwarz domain decomposition method for the conductor-like screening continuum model. *SIAM J. Num. Anal.*, 59(2):769–796, 2021.

MOX Technical Reports, last issues

Dipartimento di Matematica
Politecnico di Milano, Via Bonardi 9 - 20133 Milano (Italy)

- 50/2021** Ciaramella, G.; Vanzan, T.
On the asymptotic optimality of spectral coarse spaces
- 51/2021** Ciaramella, G.; Kwok, F.; Mueller, G.
Nonlinear optimized Schwarz preconditioner for elliptic optimal control problems
- 52/2021** Ciaramella, G.; Mechelli, L.
An overlapping waveform-relaxation preconditioner for economic optimal control problems with state constraints
- 49/2021** Rea, F.; Savaré, L.; Franchi, M.; Corrao, G; Mancia, G
Adherence to Treatment by Initial Antihypertensive Mono and Combination Therapies
- 50/2021** Rea, F.; Savaré, L; Franchi, M.; Corrao, G; Mancia, G
Adherence to Treatment by Initial Antihypertensive Mono and Combination Therapies
- 48/2021** Riccobelli, D.
Active elasticity drives the formation of periodic beading in damaged axons
- 47/2021** Orlando, G; Della Rocca, A; Barbante, P. F.; Bonaventura, L.; Parolini, N.
An efficient and accurate implicit DG solver for the incompressible Navier-Stokes equations
- 45/2021** Diquigiovanni, J.; Fontana, M.; Vantini, S.
Distribution-Free Prediction Bands for Multivariate Functional Time Series: an Application to the Italian Gas Market
- 46/2021** Diquigiovanni, J.; Fontana, M.; Vantini, F.
Conformal Prediction Bands for Multivariate Functional Data
- 44/2021** Gentili, G.G.; Khosronejad, M.; Bernasconi, G.; Perotto, S.; Micheletti, S.
Efficient Modeling of Multimode Guided Acoustic Wave Propagation in Deformed Pipelines by Hierarchical Model Reduction